ELSEVIER

Diamond and Related Materials 10 (2001) 500–505

DIAMOND AND RELATED MATERIALS

www.elsevier.com/locate/diamond

Oxygen-induced surface state on diamond (100)

J.C. Zheng[a], X.N. Xie[a], A.T.S. Wee[b], Kian Ping Loh[a,*]

[a] *Department of Chemistry, National University of Singapore, Lower Kent Ridge Road, Singapore 119260, Singapore*
[b] *Department of Physics, National University of Singapore, Lower Kent Ridge Road, Singapore 119260, Singapore*

Abstract

The electronic structure of oxygenated diamond (100) surface is studied comparatively by experimental photoemission techniques and first principles calculations. Controlled oxygenation of the diamond (100) 2×1 surface at 300°C yields a smooth O:C (100) 1×1 surface with a distinctive emission state at ~3 eV from the Fermi edge. Oxygenation of the hydrogenated surface at temperatures above 500°C, however, gives rise to extensive etching and roughening of the surface. The experimentally observed emission state at ~3 eV following O adsorption is assigned to the O-induced surface state. When the oxygenated surface is annealed to 800°C to desorb chemisorbed O, the surface structure changes from 1×1 to 2×1 and another surface state emission at 2.5 eV associated with the clean surface reconstruction can be observed by UPS. This is attributed to the π-bond reconstruction of sub-surface carbon layers following the desorption of first layer CO from the surface. To understand the origin of the O-induced emission state, we calculated the density of states (DOS) of the oxygenated diamond using the first principles linear muffin-tin orbital (LMTO) method with atomic sphere approximation (ASA) based on density functional theory (DFT) and local density approximation (LDA).

Keywords: Band structure; Density of states; Negative electron affinity; Oxygen

1. Introduction

In the last 10 years since the emergence of CVD diamond technology, there have been many detailed studies dealing with the binding characteristics and electronic properties of hydrogenated diamond [1–3], but relatively few studies to date have focused on understanding the surface properties of oxygenated diamond [4,9,10]. The presence of surface O exerts a very pronounced influence on the electronic properties of diamond. For example, the high density of space charge due to ionized gap states is found in the vicinity of the as-grown hydrogenated diamond film and disappears after oxidation [5–7]. Recently, Brandes and Mills [8] found that substantial changes in the positron yield on diamond occurred at elevated temperatures, and speculated that it may be related to surface electrons populating surface states associated with oxygen or defects. It has been suggested by Kiyota [5] as well as Gonon [6] that on an oxygen-terminated surface produced by oxygen-plasma treatment, there is a depletion layer for holes because of the presence of donor-type surface states existing at approximately 1.7 eV above the valence band. The nature of the surface state is not understood and its presence is deduced from resistivity measurements and surface photovoltage measurements. The introduction of surface states by oxygen adsorption has not been established experimentally to the best of our knowledge.

We report in this paper a detailed study of the interaction of atomic O with well-characterized diamond single crystal (100) surface. The total DOS of the

* Corresponding author. Tel.: +65-874-4778; fax: +65-779-1681.
E-mail address: chmlohkp@nus.edu.sg (K.P. Loh).

0925-9635/01/$ - see front matter
PII: S0925-9635(00)00439-8

oxygenated diamond was calculated and compared with the experimental results to verify the existence of oxygen-induced surface states.

2. Experimental

All experiments were performed in a UHV chamber with a base pressure of 1×10^{-10} torr. The sample used was a type IIb diamond single crystal (4 mm $\times$ 4 mm $\times$ 0.5 mm) that was mechanically polished in the (100) face and conductive enough to avoid charging problems during electron spectroscopy. UPS data was collected in the normal emission using either He(I) or He(II) excitation from a noble gas discharge lamp. A remote discharge RF atomic beam source was used to generate atomic beams of H or O species for interaction with the diamond surface.

3. Results and discussion

The beam nature of the remotely discharged plasma source allows investigation of the incidence angle dependence of the etching process. A smooth $1 \times 2/2 \times 1$ reconstructed face (abbreviated as 2×1) was observed to evolve from the 1×1 as-received sample following H-plasma beam treatment with the H beam applied at a glancing angle and parallel to the 110 azimuth of the sample face. Fig. 1a,b shows the RHEED pattern recorded in the 100 azimuth, and these transformed gradually into a 2×1 reconstruction over a time-span of 30 min. The 2×1 face has been verified previously by HREELS to consist of monohydride-terminated dimer rows [11]. The effect of RF-excited O atoms on the monohydride-terminated 2×1 face was investigated by exposing it to O-plasma at different substrate temperatures. The results are summarized in Table 1. The exchange of surface H by atomic O is less efficient at low temperatures (< 300°C). The change of the 2×1 face into clear 1×1 occurred at 300°C, as shown in Fig. 1c. An O coverage of approximately 0.45 monolayer (ml) coverage could be obtained at this point. At higher temperatures, rapid roughening of the surface due to extensive etching occurred and the RHEED pattern changed into a spotty pattern as shown in Fig. 1d.

A sharp final-state emission peak can be observed in the low kinetic energy end of the UPS He (I) spectra for the smooth 2×1 hydrogenated diamond surface produced by RF-hydrogen plasma beam polishing, as shown in Fig. 2a. This sharp peak is characteristic of the negative electron affinity (NEA) condition, and has been suggested to be associated with electropositive C–H bonds on the surface that effected a lowering of the vacuum level beneath the conduction band minimum (CBM) [12,13]. However, if the H:C(100) 2×1 was exposed to atomic oxygen beam at room temperature, as in Fig. 2b, the NEA peak vanished quite readily and the surface converted to a positive electron affinity condition. A coverage of 0.2 ml O is sufficient to bring about this change. The result can be rationalized in

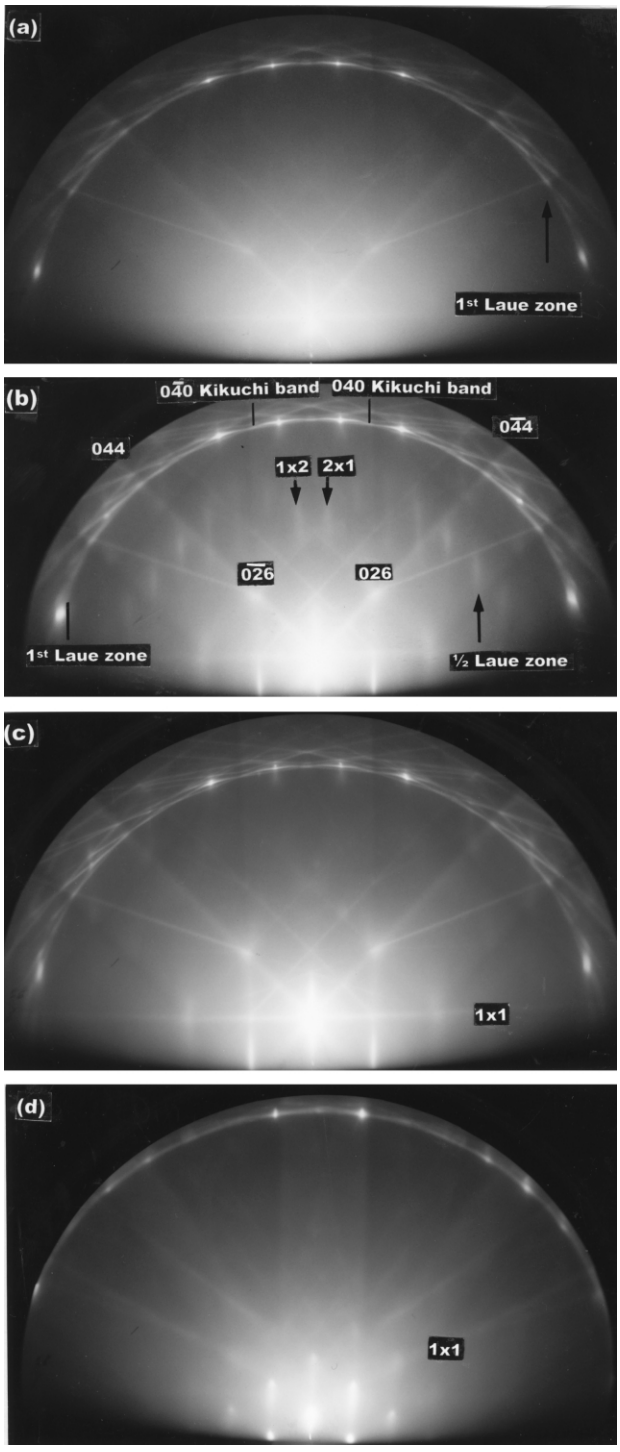

Fig. 1. Evolution of the RHEED pattern taken in the [100] azimuth following glancing-angle RF hydrogen-plasma beam etching: (a) as received; (b) after H-plasma beam treatment for 20 min; after O-plasma beam treatment at (c) 300°C for 20 min and (d) 500°C for 10 min.

Table 1
Effect of RF-excited O atoms on the monohydride-terminated 2×1 face by exposure to O-plasma at different substrate temperatures

Substrate temperature during O plasma treatment (°C)	RHEED pattern	O coverage as determined by AES/monolayer
25	Smooth 2×1	0.25
100	Smooth 2×1	0.3
200	Smooth 2×1	0.3
300	Smooth 1×1	0.45
500	Rough 1×1	0.56

terms of the electronegativity of O, because the resultant surface dipole of the C–O bonds will have the negatively polarized end facing the vacuum in contrast to the electropositive hydrogen. Fig. 2c shows the spectrum following O-plasma beam treatment at 300°C. The most significant change is the increase in valence band (VB) emission intensity at ~ 3 eV for a feature labeled 'OS' in the spectra and the continuous shift of the low-energy cut-off towards the Fermi level. The energy position of the feature 'OS' is too low to agree with the 6σ and 4π valence bands of the C=O or C–O peaks on metal or semiconductor surfaces [14,15]. The possibility that this emission state is due to the increase in the density of p-π states due to the effects of ion irradiation can be ruled out because it vanishes with the desorption of O from the surface. In addition, no evidence for the increase in p-π states can be seen in the C KLL auger lineshape. In fact, we will show later in our total DOS calculations, that this is a feature *unique* to oxygenated diamond and it is consistent with oxygen-induced surface state.

Fig. 3 shows the changes when an oxygenated 1×1 diamond surface was heated to increasingly higher temperatures. Emission state 'OS' is observed to attenuate with elevated temperatures and almost vanishes by 700°C, as shown in Fig. 3d. If the intensity of the secondary electron peak is proportional to H coverage, it can be inferred that the population of chemisorbed hydrogen on the surface has depleted considerably after the O radical beam treatment at 300°C. When the sample is annealed to 800°C, a sharper peak labeled as 'S' in Fig. 3e and which is related to clean surface reconstruction emerges [2,11,16,17]. The appearance of

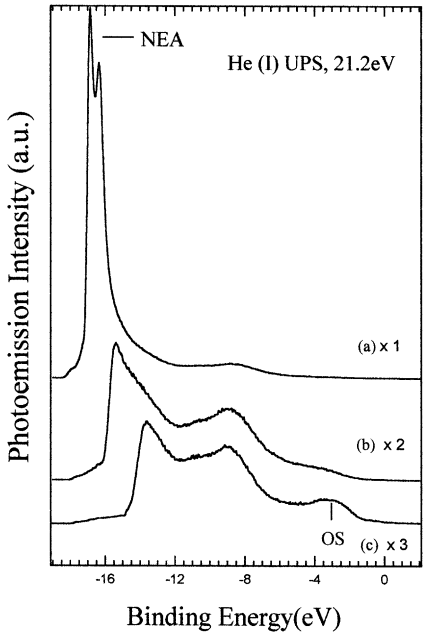

Fig. 2. UPS He (I) spectra for diamond (100) of various surface structures: (a) H:C (100) 2×1, showing strong characteristic NEA peak at 16.7 eV; (b) O: C (100) 1×1, prepared by O-plasma treatment of H:C (100) 2×1 at RT for 3 min, (c) O-plasma treatment for 20 min at 300°C. Note the emergence of the O-related surface state peak labeled as 'OS' in the spectra.

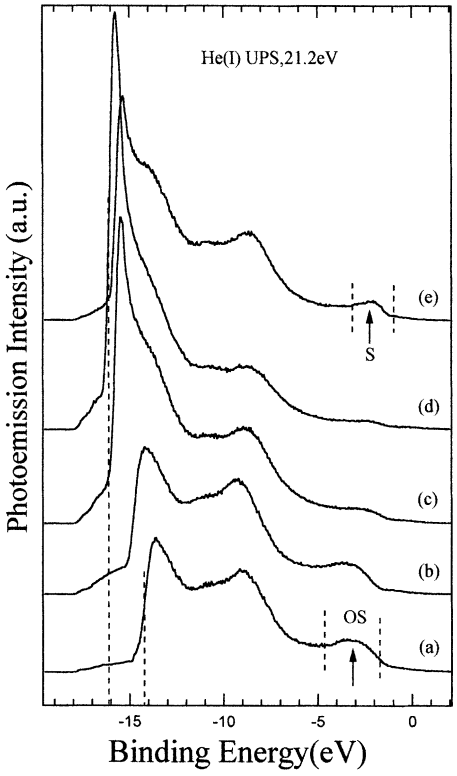

Fig. 3. UPS He (I) spectra for diamond (100) 1×1 obtained after (a) O-plasma beam treatment at 300°C; and after successive annealing to (b) 300°C; (c) 500°C; (d) 700°C and (e) 850°C. Note the emergence of the surface state peak at 2.5 eV after the attenuation of the O-related surface state peak at 3 eV.

peak 'S' was accompanied by the simultaneous appearance of a clear 2×1 RHEED reconstruction. The formation of peak 'S' at 800°C is believed to arise from the spontaneous π-bond formation of the second layer subsurface carbon after the desorption of the first layer as CO or CO_2 [9,10]. The lower annealing temperatures needed for producing this surface state in the case of the oxygenated diamond is due to the lower desorption temperatures (800–1000°C) of CO_x species from the surface [10] compared with chemisorbed H. The 1×1 to 2×1 transition can be re-cycled several times without observing any degradation in surface crystallinity.

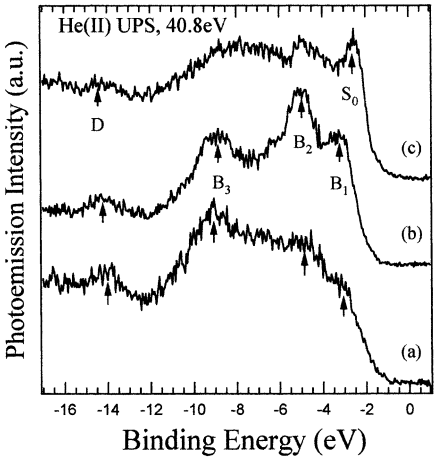

Fig. 4. UPS He (II) spectra for O:C (100) 1×1 with (a) 0.2 ml O coverage (b) 0.45 ml O coverage (c) after annealing to 800°C, a 2×1 structure results.

4. Density of states (DOS) of oxygenated diamond(100) surface from first principles theory

The He(II)-excited spectra of the oxygenated diamond surfaces are displayed in Fig. 4a,b, corresponding to surfaces with 0.2 and 0.45 ml of O respectively. The 0.2 ml O: C(100) 1×1 surface was prepared by exposing the H:C(100) 2×1 surface to oxygen radical beam at room temperature, whilst the 0.46 ml O:C (100) 1×1 surface was prepared by increasing the substrate temperature to 300°C during the treatment. Fig. 4a,b shows several distinct peaks (OS, B_1 and B_2) that mirror the integrated occupied DOS. Fig. 4c shows the valence band structure of the clean, reconstructed 2×1 surface which has a lineshape that is quite different to that of the oxygenated surfaces. A sharp state labeled as S_o related to the clean surface π-bond reconstruction is observed, analogous to the surface state peak in the He(I) spectrum shown previously in Fig. 3e.

4.1. Computational method

The DOS of the oxygenated diamond (100) surface was calculated using the linear muffin-tin orbital (LMTO) method in the atomic-sphere approximation (ASA). This method is based on the density functional theory in the local density approximation (LDA). The calculation involved the use of a supercell of a nine-layer diamond slab (both side of the slab covered by 1 layer of oxygen) separated by a vacuum region. Two models of oxygenated diamond (100) surface were used in this work, i.e. bridging structure (C–O–C) and double-bonded structure (C=O, oxygen on-top structure). In this work, we used a bond length of 1.45 Å for C–O in bridging structure, and a bond length of 1.25 Å for C=O in doubled-bonded structure. The optimized theoretical lattice constant of bulk diamond structure, i.e. 3.562 Å was used as the lattice constant [18]. For bulk diamond, 182 special k points were used in the self-consistent calculation as well as calculation of density of states. For oxygenated diamond (100) surface (slab), three special k points [19] in the irreducible Brillouin zone were used for the (001) slab for self-consistent calculations in this work, i.e. (π/a) (1/4, 1/4, a/2c) (weight = 1/4), (π/a) (3/4, 3/4, a/2c) (weight = 1/4), (π/a) (3/4, 1/4, a/2c) (weight = 1/2). 252 k points were used for the calculation of the density of states.

In Fig. 5, we show the band structure of diamond along several symmetry directions. The computational result shows an indirect band gap. The CBM is located at approximately (2π/a) (0.8, 0.0, 0.0), this agrees well with experiments. The VB width (absolute energy difference of Γ_{25} and Γ_1) of diamond calculated in this work is 21.71 eV, which is in excellent agreement with the value of 21.63 eV calculated from the linearized augmented plane wave method (LAPW) [20] and also

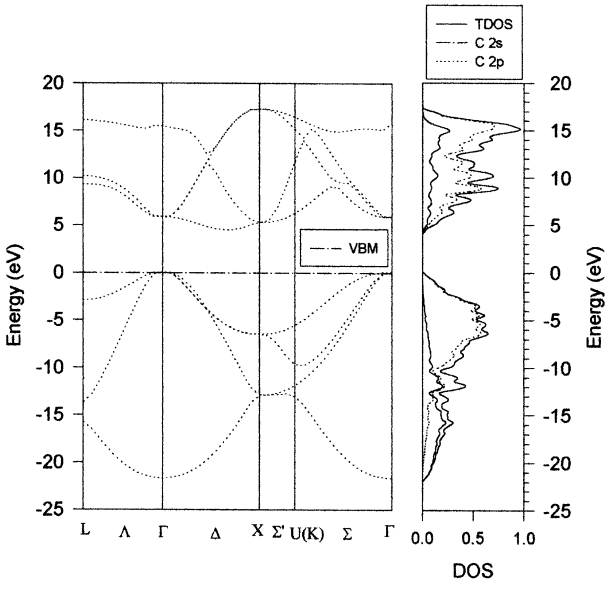

Fig. 5. Band structure and the total DOS with s and p partial density of states of diamond calculated by first principles LMTO-ASA.

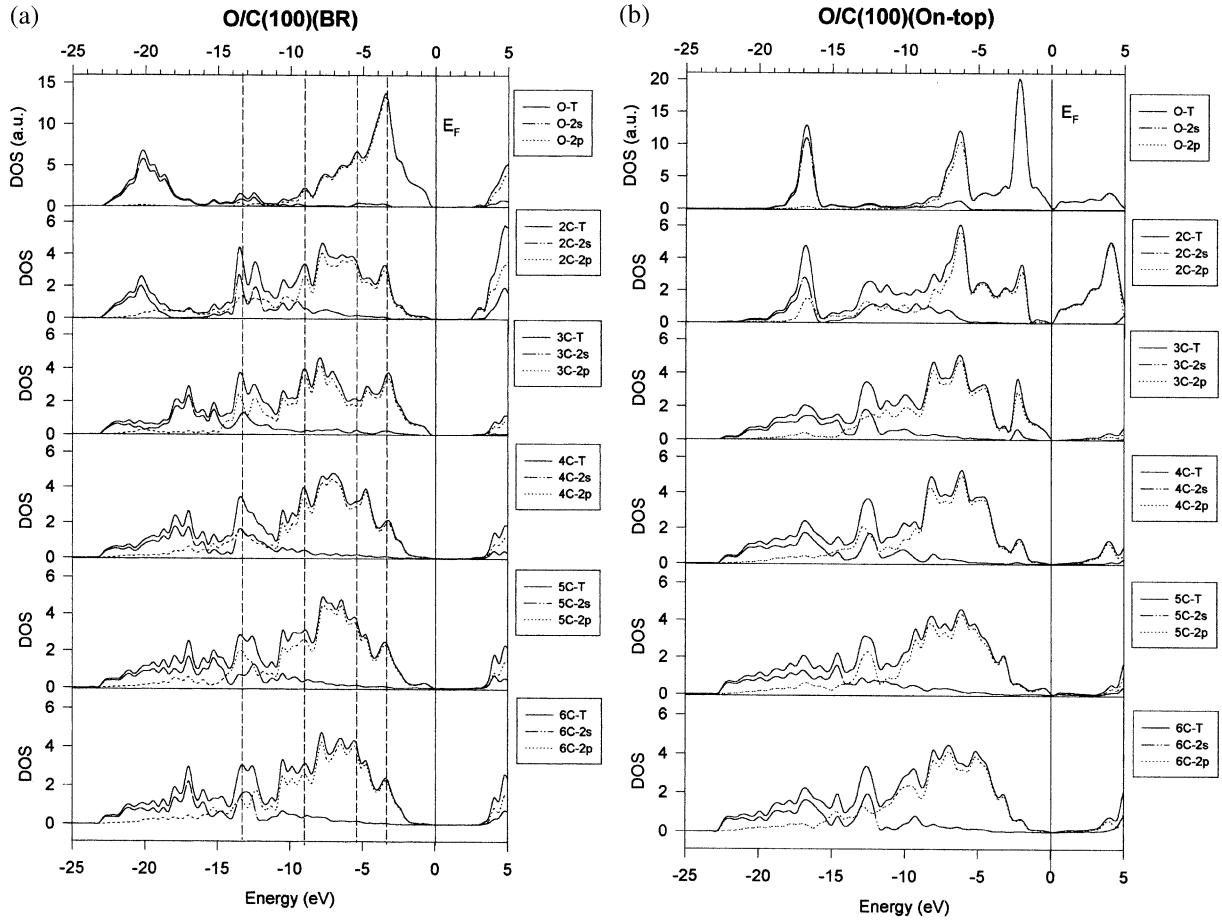

Fig. 6. (a) LPDOS of the BR model of oxygenated diamond (100) surface. (b) LPDOS of the OT model of oxygenated diamond (100) surface.

with the photo-emission results of 21.0 ± 1.0 eV [21]. Our calculated width is within the experimental error. Our calculated value of band gap E_g for diamond is 4.2 eV using LDA, which agrees well with the results (4.15 eV) obtained by other self-consistent method with LDA [20,22]. These values are lower than the experimentally determined value 5.5 eV [20] because the LDA method underestimates the fundamental gap. One way to improve the band gap is using the so-called GW approach. With the GW correction of approximately 1.53 eV [22], we can obtain the corrected band gap value of 5.7 eV, which agrees reasonably well with the measured value.

The features of the occupied states are reflected in the corresponding density of states of the VB. The calculated s and p partial DOS of diamond, as well as the total DOS from our LMTO-ASA band structure is also shown in Fig. 5. The broad peak in the calculated spectrum at -5 eV consists mainly of 2p-states. The peak at -12 eV originates from hybridized 2s and 2p states. The lowest energy peak (~ -16 eV) is dominated by 2s states.

The calculated layer projected density of states (LPDOS) of oxygenated diamond surface with surface atoms adopting the 'bridging (BR) model' and 'on-top (OT) model' are shown in Fig. 6a and Fig. 6b respectively. Each spectrum corresponds to an atomic layer starting from the O layer on the top. The TDOS of both models shows significant oxygen-induced surface states between -2.2 to -3.4 eV, and several bulk-like peaks (e.g. the peak located at ~ -13 eV). In the BR model, the 2p state peak is located at -3.4 eV. In the OT model, however, this peak splits into two peaks at -2.2 eV and -6.2 eV, respectively. Chemical bonding of first layer carbon with oxygen strongly affects the LPDOS of subsequent carbon layers. The stronger intensity of the surface state emission in the OT model compared to the BR model is due to the strong dipole polarization effect of C=O bonds on diamond surface.

5. Conclusions

We have demonstrated that the atomic beam treatment (H and O) of diamond surfaces in high vacuum conditions constitutes a controlled way to prepare a smooth hydrogenated 2×1 surface or oxygenated 1×1 surface. The adsorption of O results in the emergence

of a surface state peak at ~3 eV from the Fermi level. First principles calculations using the LMTO approach confirm the existence of oxygen-induced surface states. Differences exist in the total DOS for two types of oxygenated surface — the 'bridging' (BR) model and the 'on-top' (OT) model. In the BR model, the surface state peak is located at −3.4 eV from the Fermi level. In the OT model, however, this peak splits into two peaks at −2.2 eV and −6.2 eV respectively.

References

[1] T. Aizawa, T. Ando, M. Kamo, Y. Sato, Phys. Rev. B 48 (1993) 18348.
[2] R. Graupner, M. Hollering, A. Ziegler, J. Ristein, L. Ley, Phys. Rev. B 55 (1997) 10841.
[3] Y.M. Wang, K.W. Wong, S.T. Lee et al., Phys. Rev. B 59 (1999) 10347.
[4] R. Klauser, J.M. Chen, T.J. Chuang, L.M. Chen, M.C. Shih, J.C. Lin, Surf. Sci. 356 (1996) L410–416.
[5] H. Kiyota, H. Okushi, T. Ando, M. Kamo, Y. Sato, Diamond Relat. Mater. 5 (1996) 718.
[6] P. Gonon, A. Deneuville, E. Gheeraert, F. Fontaine, Diamond Relat. Mater. 3 (1994) 729.
[7] J. Shirafuji, T. Sugino, Diamond Relat. Mater. 5 (1996) 706.
[8] G.R. Brandes, A.P. Mills, Jr., Phys. Rev. B 58 (1998) 4952.
[9] M.Z. Hossain, T. Kubo, T. Agura et al., Surf. Sci. 436 (1999) 63.
[10] R.E. Thomas, R.A. Rudder, R.J. Markunas, J. Vac. Sci. Technol. A 10 (1992) 2451.
[11] B.D. Thoms, J.E. Butler, Surf. Sci. 328 (1995) 291.
[12] C. Bandis, B.B. Pate, Phys. Rev. B 52 (1995) 12056.
[13] T.P. Humphreys, R.E. Thomas, D.P. Malta et al., Appl. Phys. Lett. 70 (1997) 1257.
[14] Y. Bu, M.C. Lin, Surf. Sci. 298 (1993) 94.
[15] W. Kirstein, I. Petraki, F. Thieme, Surf. Sci. 331 (1995) 162.
[16] G. Francz, P. Oelhafen, Surf. Sci. 329 (1995) 193.
[17] J. Wu, R. Cao, X. Yang, P. Pianetta, I. Lindau, J. Vac. Sci. Technol. A 11 (1993) 1048.
[18] J.C. Zheng, C.H.A. Huan, A.T.S. Wee et al., J. Phys.: Condens. Matter 11 (1999) 927.
[19] S.H. Ke, K.M. Zhang, X.D. Xie, Phys. Rev. B 55 (1997) 512.
[20] C.Y. Fong, B.M. Klein, Electronic and vibrational properties of bulk diamond, in: L.S. Pan, D.R. Kania (Eds.), Diamond: Electronic Properties and Applications, Kluwer, Dordrecht, 1995.
[21] J. Himpsel, J.F. van der Veen, D.E. Eastman, Phys. Rev. B 22 (1980) 1967.
[22] P. Surh, S.G. Louie, M.L. Cohen, Phys. Rev. B 45 (1992) 8329.